Submitted Manuscript

Applied Spectroscopy
www.s-a-s.org

Disease-Associated Multimolecular Signature in the Urine of Patients with Lyme Disease Detected Using Raman Spectroscopy and Chemometrics

Applied Spectroscopy
2022, Vol. 0(0) 1–16

DOI: 10.1177/00037028211061769
journals.sagepub.com/home/asp
SAGE

Ryan S. Senger[1,2], Amr Sayed Issa[2], Ben Agnor[1], Janine Talty[3], Alicia Hollis[4], and John L. Robertson[2,5]

Abstract

A urine-based screening technique for Lyme disease (LD) was developed in this research. The screen is based on Raman spectroscopy, iterative smoothing-splines with root error adjustment (ISREA) spectral baselining, and chemometric analysis using Rametrix software. Raman spectra of urine from 30 patients with positive serologic tests (including the US Centers for Disease Control [CDC] two-tier standard) for LD were compared against subsets of our database of urine spectra from 235 healthy human volunteers, 362 end-stage kidney disease (ESKD) patients, and 17 patients with active or remissive bladder cancer (BCA). We found statistical differences ($p < 0.001$) between urine scans of healthy volunteers and LD-positive patients. We also found a unique LD molecular signature in urine involving 112 Raman shifts (31 major Raman shifts) with significant differences from urine of healthy individuals. We were able to distinguish the LD molecular signature as statistically different ($p < 0.001$) from the molecular signatures of ESKD and BCA. When comparing LD-positive patients against healthy volunteers, the Rametrix-based urine screen performed with 86.7% for overall accuracy, sensitivity, specificity, positive predictive value (PPV), and negative predictive value (NPV), respectively. When considering patients with ESKD and BCA in the LD-negative group, these values were 88.7% (accuracy), 83.3% (sensitivity), 91.0% (specificity), 80.7% (PPV), and 92.4% (NPV). Additional advantages to the Raman-based urine screen include that it is rapid (minutes per analysis), is minimally invasive, requires no chemical labeling, uses a low-profile, off-the-shelf spectrometer, and is inexpensive relative to other available LD tests.

Keywords

Raman spectroscopy, chemometric analysis, Lyme disease, discriminant analysis, baseline algorithms

Introduction

Lyme disease (LD) in North America is caused by infection with the spirochete, *Borrelia burgdorferi sensu lato*, a pathogen transmitted through bites from ixodid ticks.[1–4] A second pathogen, *Borrelia mayonii*, has also been associated with some LD cases in North America. Other species of *Borrelia* are associated with LD in Europe and Asia.[5] Ixodid tick vectors, capable of transmitting *B. burgdorferi* and several other diseases, for example, tick-borne relapsing fever (TBRF), *Borrelia miyamotoi or Borrelia hermsii*, are present worldwide.[6,7] Wildlife hosts, such as deer and mice, play an important role in disease transmission. Domesticated animals (horses, cattle, dogs, and cats) may show serologic reactivity to *B. burgdorferi* antigens and may also develop clinical signs of acute and chronic LD, although most infections may be inapparent.[8–11] The role of domesticated animals in supporting/fostering transmission of LD is unknown.

The pathophysiology, clinical course, and treatment of LD have been described in many excellent reviews spanning more than four decades. The interested reader, seeking more information, will be well served by reading them.[2,12–14]

The spread of LD from the northeastern United States, across the north, central, and southeastern United States, and

[1]Department of Biological Systems Engineering, Virginia Tech, Blacksburg, Virginia, USA
[2]DialySensors Inc., Blacksburg, Virginia, USA
[3]Neuromusculoskeletal Medicine & OMM, Roanoke, Virginia, USA
[4]Valley Integrative Medicine, Roanoke, Virginia, USA
[5]Department of Biomedical Engineering and Mechanics, Virginia Tech, Blacksburg, Virginia, USA

Corresponding author:
John L. Robertson, Department of Biomedical Engineering and Mechanics, Virginia Tech, 325 Stanger St., Blacksburg, VA 24061, USA.
Email: drbob@vt.edu

into southern Canada, has been a cause of both public health and economic concern.[6,15–20] The costs of diagnosis, treatment, and loss of productivity continue to grow. Hinckley and co-workers[21] estimated that the cost of LD diagnostic testing alone, using 2008 data from large commercial laboratories, was more than US$492 million.

The diagnosis of acute LD (3–30 days after tick bite) is based on clinical evaluation of patients with post-exposure rash (erythema migrans), headache, moderate to severe acute-onset arthritis, fatigue, myalgia, and serologic confirmation of infection. Not all patients with serologic confirmation of infection show any or all of these signs[22] and the severity of clinical signs (if present) is highly variable.

Some physicians, faced with deciding whether or not to treat a patient for LD solely on the basis of clinical signs, but without serologic confirmation, opt for treatment with antibiotics.[23] Antibiotics are sometimes offered to patients who seek treatment for chronic fatigue, intermittent or persistent pain, and/or neurocognitive dysfunction, among other symptoms; this is controversial (see below). Some patients believe they may be suffering from "chronic LD", a clinical syndrome for which there is no precise definition, diagnostic test, or definitive immediate response to appropriate antibiotic therapy.[16,24,25]

Recently, Kobayashi et al.[26] questioned the wisdom of widespread prescription of antibiotic therapy. They reported that more than 70% of patients referred with "LD" to an academic infectious disease clinic were considered misdiagnosed and >80% of those patients were considered to have received unnecessary antimicrobial therapy. In contrast, another recent study,[27] using data from a patient-derived database,[28] showed that some patients experienced significant benefits from a combination of antibiotic and alternative therapies, and focused medical management.

In 2017, the Centers for Disease Control and Prevention[7] reported nearly 43 000 LD cases, based on laboratory confirmation or clinical diagnosis by physicians (discussed more fully, below). Researchers estimate that the number of actual cases is significantly higher (>300 000 per year)[21] when extrapolating from laboratory submissions and clinical reports. This estimate was based on more than 3.4 million tests for LD infection performed annually (on approximately 2.4 million specimens), with positive results from two-tiered serologic testing (see below), showing infection in approximately 10–18% of patients.

Laboratory confirmation of LD infection is commonly done with two-stage serology (enzyme immunoassay, followed by Western immunoblot assay) in which antibody titers against *B. burgdorferi* antigens are compared from acute and convalescent sera.[22,29] This is widely considered the definitive procedure for LD diagnosis. The accuracy of the recommended serologic assays is dependent on timely elaboration of antibodies, specifically to the *B. burgdorferi* pathogen. The development of antibodies, however, may take several weeks in patients with clinical signs, and reliance on serology alone may delay disease recognition or treatment. In some patients with a slow or minimal serologic response, those with persistence of antibodies from distant exposure/past infection, or potential cross-reactivity with other antigens/tick-borne diseases, the confirmation of LD infection through serology alone may be problematic.[5,25,30]

Other tests for LD have been developed and used, but the relevance, accuracy and value of such tests has been questioned and considered unsupported by objective, robust, and correlative (clinical symptoms/laboratory data) studies.[5] Correlations of chronic LD with decreased CD57 lymphocyte levels have been noted,[31,32] but these have also been reconsidered more recently.[33] Advances in serodiagnostic methods, combined with state of the art molecular technologies, hold the promise of more accurate and timely LD diagnosis.[34,35] However, no current test has been widely accepted as a suitable replacement for the recommended two-stage serologic assay on acute and convalescent sera.[30,36–38]

Recently, Pegalajar-Jurado et al.,[39] building on both positive and negative results from previous urinalysis studies,[40–42] described detection of urinary metabolites/biomarkers associated with early LD infection, in specimens of 14 early LD patients, using liquid chromatography mass spectroscopy (LC-MS) based methods. Comparing the urine metabolome of 14 patients with infectious mononucleosis and that of 14 healthy human volunteers, they found dysregulation of multiple metabolic pathways (including the tryptophan pathway) that they considered signatory (71–100% accurate, depending on the pathway and comparison population) for early LD. With additional studies and verification, these proof-of-concept studies suggest strongly that a urine-based test for LD is entirely possible.

It is clear that there is a pressing need, given the increased incidence of LD, to evolve diagnostic tests that are rapid, inexpensive, relevant, and potentially noninvasive (most current methods require blood/serum). Such tests must be supported by objective evidence of high positive and negative predictive value, specifically for LD, while excluding myriad other causes of chronic LD.

Here, we describe the results of a study of urine specimens, analyzed using Raman spectroscopy and chemometric analyses, from patients testing positive for LD with a host of serologic tests. These patients are referred to as "LD-positive" throughout the description of this study. LD-positive patient urine spectra (n = 30) were compared with subsets of our urine spectra database containing 235 spectra of healthy human volunteers,[43] 362 patients with end-stage kidney disease (ESKD),[44] and 56 patients with active or remissive bladder cancer (BCA),[45] The analysis was carried-out using Rametrix methods and software,[46,47] and we also explored the use of iterative smoothing-splines with root error adjustment (ISREA)[48] for baselining Raman spectral data compared it to the Goldindec algorithm,[49] which was used in our previous studies.

We hypothesized that LD-positive patients would have a distinctive multimolecular signature in urine that could be

detected with Raman spectroscopy and chemometric analyses. Once this hypothesis was proven valid, we then explored the accuracy, including sensitivity, specificity, positive predictive value (PPV), and negative predictive value (NPV) of the Raman-based urine screen for the presence of LD. This urine screen was then applied to the urine spectra of patients displaying LD symptoms who either had not taken a two-tiered serologic test or had a negative two-tier serologic test result, even though some of these patients had exhibited a low CD57 natural killer cell (NK) count (<60) (not considered by many to indicate LD).

Methods

Patients and Controls

Informed Consent. Informed consent for the collection of urine specimens (Protocol: VT IRB no. 15-703) was obtained and 15–30 mL of voided, mid-stream urine was collected in sterile specimen containers and frozen (−35 °C) until retrieved for analysis, at which point specimens were warmed to 25 °C and analyzed (see below)

Patients. Eighty-five patients were seen by two primary care specialists (JT, AH) for evaluation of chronic fatigue/related issues, potentially indicative of infection with *B. burgdorferi* or exposure to environmental contaminants such as molds. The patient population consisted of 59 female and 26 male patients. The age range of female patients was 2–74 years and of male patients 17–74 years. As would be expected, the clinical presentation of patients was highly variable, as was the duration and severity of clinical symptoms. Many patients had pursued multiple avenues of diagnosis and variable courses and types of therapies (including antibiotics) prior to evaluation.

Of these patients, 30 tested positive for LD with serologic tests. Of this group, 14 tested positive with the CDC serologic test. No patients evaluated had erythema migrans at the time of presentation. A majority of patients were also evaluated with other types of testing for LD (not CDC serologic testing) or to screen for the presence of other disease entities, including LD tests from iGeneX, iGene, iSPOT, LabCorp, and/or Quest. As noted previously (see above), the value and acceptance of results of these tests is debatable.

Controls: Healthy Volunteers. A full analysis of the healthy human volunteer urine dataset has been published.[43] Briefly, 235 urine specimens were collected from 48 (39 females, nine males) healthy human volunteers with no history or evidence of renal disease. Volunteers were also free of infectious or degenerative disease at the time of sample collection. The age range of the healthy volunteer population was 18–70 years; 87.5% of volunteers were of ages 19–22 years, and the median age was 21 years. From this dataset, 185 urine spectra were selected randomly and a subset of 30 were used in this study.

Controls: End-stage Kidney Disease Patients. A full analysis of the ESKD patient urine dataset has been published.[44] In total, 362 urine specimens were collected from 96 patients. Patients had advanced ESKD were undergoing treatment with ambulatory peritoneal dialysis (PD). Patients ranged in age from 24–90 years old. The mean age was 60 years, and the median age was 63.5 years. Multiple urine specimen collections (four to eight separate collections) were available from multiple patients, allowing repetitive measurements and correlations over a protracted course of PD therapy (18 months). From this dataset, 30 urine spectra were selected randomly and used in this study.

Controls: Bladder Cancer (BCA) Patients. A full analysis of the BCA patient urine has also been published.[45] In total, 56 urine specimens (one per patient) were collected. The patients ranged in age from 31–91 years old. The mean and median age of 62 years. Of this dataset, 17 specimens were from patients with active bladder cancer. The median age of this population was 70 years. In addition, 17 of these specimens were selected randomly, among the patients with active BCA at time of collection, and used in this study.

Analytical Standards. Surine urine negative control (Dyna-Tek Industries, USA) was used as a control standard for urinalysis.

Specimen Collection and Storage

Voided, mid-stream urine specimens were collected and transferred into sterile specimen cups and then immediately frozen to −15 °C and then stored at −35 °C until analyzed.

We previously determined the suitability of collection and storage conditions in a separate study of urine stability[45] and adhered to the guidelines set forth in that study. Unused portions of urine and spent dialysate specimens were stored at −35 °C for the duration of the study and re-analyzed, as needed.

Raman Methodology and Measurements

Previously published experimental methods were used[43–45] and are described here. All stored urine specimens were thawed, equilibrated to room temperature, and transferred to 2 mL screw thread flat bottom borosilicate glass vials (Fisher Scientific). An Agiltron PeakSeeker Pro-785 dispersive Raman spectrometer was used with a liquid vial holder (attached *via* fiber optic cable) to scan all samples in bulk liquid configuration. All scans were performed at 25 °C using a 785 nm laser, 30 s excitation time, 30 mW laser power, 0.2 mm laser spot size, over a 200–2000 cm^{-1} range, and spectral resolution of 8 cm^{-1} (manufacturer default). A minimum of 10 scans were collected per vial and averaged. Spectral data were collected with RSIQ software, and resulting spectral files contained Raman signal intensity values per 1 cm^{-1}.

Computational Methodology

Previously published computational methods were also used.[43–47] Spectral processing and analyses were performed with the Rametrix Lite v1.1,[46] Rametrix Pro v.1.0,[47] and the Statistics and Machine Learning Toolboxes with Matlab r2018A (The MathWorks, Inc., USA). In Rametrix Lite, Raman spectra were truncated to Raman shifts of 600–1800 cm^{-1}, baseline corrected using both the Goldindec algorithm[49] and ISREA,[48] and vector normalized. For Goldindec baselining, the following parameters were used: Third-order polynomial, estimated peak ratio of 0.5, and smoothing window size of five. Adjustments were made with the ISREA regarding where nodes were placed in the spectra. These nodes (i.e., also called "knots") are used to connect cubic splines for baselining.[48] Wavenumber calibration was performed by using the dominant urea Raman shift (adjusted to 1002 cm^{-1}) in urine as a reference point. Principal component analysis (PCA) and discriminant analysis of principal components (DAPC) models were also constructed with the Rametrix Lite Toolbox. The DAPC models were tested by leave-one-out analysis with the Rametrix PRO Toolbox, as has been described and demonstrated.[43–45,47] This procedure allowed calculation of the test accuracy, sensitivity, specificity, PPV, and NPV. These have also been defined in previous publications,[45,50] and here, the CDC serologic test is treated as the "gold standard" when comparing to the Rametrix urine screen. The urine screen accuracy is the percentage of spectra that were assigned to the correct group when treated as the "unknown" in the leave-one-out analysis. The sensitivity describes the percentage of patients that test positive by the gold standard test that then go on to test positive by the urine screen. The specificity is the percentage of patients that test negative by the gold standard test that then go on to test negative by the urine screen. The positive predictive value (PPV) is the percentage of patients that screen positive by the urine screen that then go on to test positive by the gold standard test. Finally, the negative predictive value (NPV) is the percentage of patients that screen negative by the urine screen that then go on to test negative by the gold standard test.

Statistical comparisons of spectra were performed with one-way analysis of variance (ANOVA) and pairwise comparisons using Tukey's honestly significant difference (HSD) procedure in Matlab. The following analysis was performed with un-averaged Raman scans of the entire dataset. Spectra were truncated to 600–1800 cm^{-1}, baselined with Goldindec or ISREA, and vector normalized. These spectra were reduced to single-value entities by calculation of the total spectral distance (TSD) and total principal component distance (TPD) by comparison with the urine analytical standard Surine. The calculation of TSD and TPD for statistical analyses has been described in the literature,[43–45] and the calculations are herein described briefly. For the calculation of TSD, the distance between a patient urine spectrum (e.g., an LD-positive patient or healthy volunteer) and an analytical reference standard (i.e., Surine) was calculated at every Raman shift and summed over all Raman shifts (i.e., 600–1800 cm^{-1}). For the TPD, the distance between the top five principal components (PCs) was calculated between a patient urine spectrum and a reference spectrum. ANOVA and pairwise comparisons were then performed on these TSD and TPD calculated values.

Study Targets

We performed multiple analyses to test our hypothesis, "patients with LD have a distinctive multimolecular signature in urine that can be detected with Raman spectroscopy and Rametrix". In doing so, we asked the following questions:

Are Raman spectra of urine from LD-positive patients statistically different from urine spectra from healthy volunteers?

(ii) Are the urine spectra of patients testing LD-positive with the CDC serological test statistically different from those of patients who tested positive with a non-CDC test?

(iii) Are the urine spectra of patients who tested LD-positive with a serological test different from those who tested LD-negative but had low CD57 NK counts (<60)?

(iv) Are the urine spectra of LD-positive patients statistically different from those who tested LD-negative?

(v) How would a Rametrix-based urine screen perform when constructed with urine spectra from LD-positive patients and healthy volunteers?

(vi) What molecules (i.e., "molecular signature") distinguish LD-patient urine from that of healthy volunteers?

(vii) How would a Rametrix-based urine screen perform when constructed with urine spectra from LD-positive patients, healthy volunteers, and patients with ESKD or BCA?

(vi) What percentage of those patients with symptoms resembling LD and either no serological test history or an LD-negative serological test would screen positive with this Rametrix-based urine screen?

Results

Raman Spectra of Individual Patient Groups

A summary of the patients, urine specimens collected and used, and dataset groupings used in this study are given in Table I. Raman spectra from all patient groups and the urinalysis standard Surine were processed with the Rametrix Lite Toolbox v.1.1 for Matlab, as described previously. The urine spectra were averaged for each group following truncation (600–1800 cm^{-1}), baselined with Goldindec and ISREA, and vector normalized. Two sets of nodes were used with ISREA

Table I. A summary of patients, urine specimens, and group assignments used in this study.

Description	Number of urine specimens collected and used in this study	Assigned group name in this study	References for urine specimens
Patients with symptoms resembling LD and no serologic test results	41	No-test	This study
Patients with symptoms resembling LD and a negative serologic test	13	Neg-test	This study
Patients with positive serologic test (CDC, iGeneX, iGene, iSPOT, LabCorp, and/or Quest)	30	LD-positive	This study
Patients with positive CDC serologic test[a]	14	CDC-LD-positive	This study
Patients with positive iGeneX test only	11	Other-LD-positive	This study
Patients with positive iGene or iSPOT test only	2	Other-LD-positive	This study
Patients with positive LabCorp or Quest test only	3	Other-LD-positive	This study
Patients with CD57 NK count only (value <60) and no other positive test[b]	11	CD57	This study
Healthy volunteers	30 (of 235 total)	Healthy	Published[43]
Patients with ESKD	30 (of 362 total)	ESKD	Published[44]
Patients with active BCA	17	BCA	Published[45]
Healthy volunteers, patients with ESKD; patients with active BCA	77	LD-negative	This study
Surine urine analytical standard	1	Surine	Published[43–45]

[a]Patients testing positive with the CDC serologic test and one or more other tests were grouped using the CDC-LD-Positive dataset.
[b]One patient presenting with symptoms resembling LD was found to have a CD57 NK count of 68. This patient was included in the group.

in this study and are given in Table II. The processed representative spectra are shown in Figure 1 for Goldindec and ISREA node set number (no.) 1 baselining, and the differences arising from the different baselining algorithms is clear. Similar spectra for ISREA node set no. 2 are given in the Supplemental Material (Figure S1). Also apparent from visual inspection of representative spectra is that the urine spectrum of LD-positive patients more closely resembles the spectrum of healthy human volunteers (with both Goldindec and ISREA) than the urine spectra of either ESKD or BCA patients. Subtle differences between the LD-positive representative spectrum and that of healthy volunteers were observed at 1002 cm^{-1} (representative of urea), around 900 cm^{-1}, and from 1200–1400 cm^{-1} (all commonly associated with tryptophan and protein, including collagen).[51] However, these subtle differences were both subjective and insufficient to identity the presence of LD in urine through simple visual inspection alone. Thus, Rametrix computational tools were needed to perform a chemometric analysis of the spectra to discover defining characteristics (i.e., the "molecular signature") of LD in urine.

Table II. ISREA nodes used in this study.

ISREA node set	Node locations (cm^{-1})
Node set no. 1	600, 800, 900, 1100, 1200, 1400, 1600, 1800
Node set no. 2	600, 617, 947, 962, 1249, 1378, 1410, 1800

Statistical Comparisons Among Groups of Urine Raman Spectra

For the responses to Questions 1–4 below, TSD and TPD values were generated as described in the Methods section with the Surine scan as the control. Calculations were performed for spectra baselined with Goldindec, ISREA with node set no. 1, and ISREA with node set no. 2 separately. TPD calculations were performed using five PCs. In all cases, one-way ANOVA of the entire scan dataset was performed, followed by pairwise comparisons with Tukey's HSD procedure. A total of six pair-wise comparison *p*-values were calculated for each analysis (i.e., TSD, TPD, with three baselines each). All *p*-values of pairwise comparisons are given in Table S1 (Supplemental Material).

Question 1: Are Raman Spectra of Urine From Lyme Disease-Positive Patients Statistically Different From Urine Spectra From Healthy Volunteers?

The groups of urine spectra LD-Positive and Healthy in Table I were used to answer this question. All pairwise comparisons from TSD data revealed statistical significance ($p < 0.001$) between the groups. Two of three TPD calculations also showed the same level of statistical significance. Only the TPD calculation with Goldindec showed less significance ($p = 0.055$). Given this, the calculations suggest that real molecular differences may exist between the two groups that can be elucidated by chemometric analysis.

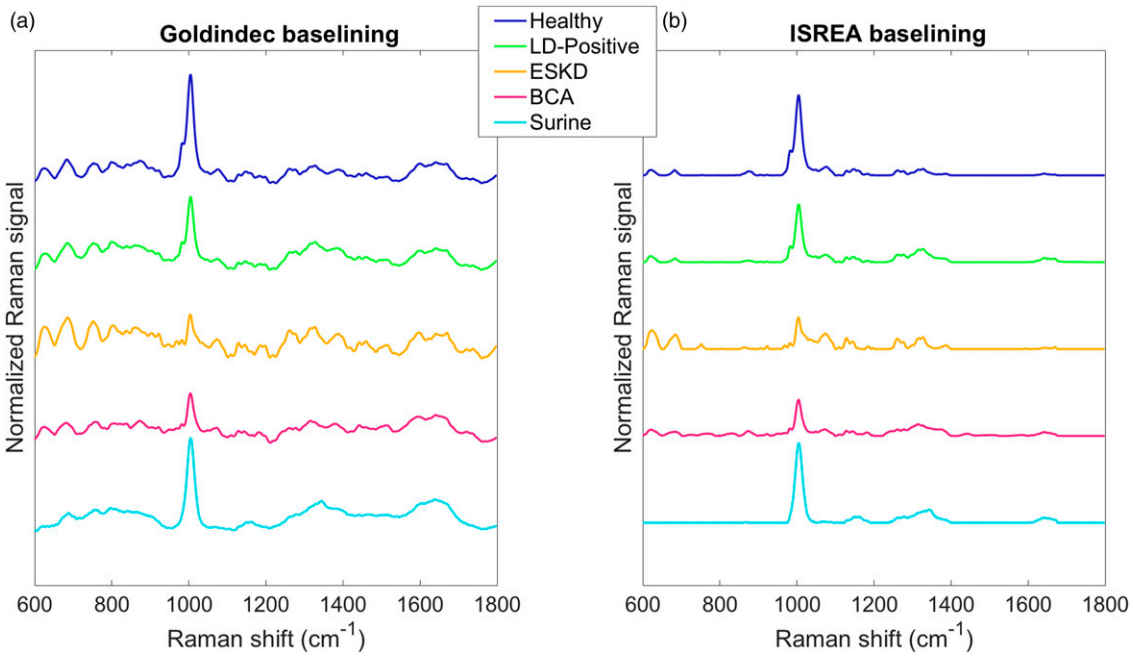

Figure 1. Representative baselined and normalized spectra given (a) Goldindec and (b) ISREA baselining with node set no. 1.

Question 2: Are the Urine Spectra of Patients Testing Lyme Disease-Positive With the Centers for Disease Control Serological Test Statistically Different From Those of Patients Who Tested Positive With a Non-Centers for Disease Control Test?

The same procedure was applied to the CDC-LD-Positive and Other-LD-Positive groups, defined in Table I, to test if there was any significant difference in the urine spectra of patients who tested LD-positive by different tests. All pairwise comparisons suggested no statistically significant differences exist between these groups (i.e., all p-values > 0.05). It is noted the TPD data with Goldindec baselining was $p = 0.059$. Overall, results from these analyses confirmed that the CDC-LD-Positive and Other-LD-Positive groups could be grouped together as LD-Positive and used in further calculations.

Question 3: Are the Urine Spectra of Lyme Disease-Positive Patients Statistically Different From Those Who Tested Lyme Disease-Negative?

The procedure was applied to the LD-Positive and Neg-Test groups of Table I. All pairwise comparisons with TSD data suggested no statistical differences between these groups ($p > 0.05$). Of the pairwise comparisons with TPD data, those with Goldindec and ISREA node set no. 1 suggested statistically significant differences between the groups ($p < 0.001$), while the TPD data with ISREA node set no. 2 returned $p = 0.56$. Thus, it was inconclusive whether these groups were different, based on these analyses. This suggests that some urine specimens of the Neg-Test group could have the LD molecular signature. Individual specimens were analyzed for this using our Raman-based screen and chemometric analysis, and results are reported in a later section.

Question 4: Are the Urine Spectra of Lyme Disease-Positive Patients Statistically Different From Those With No Lyme Disease-Positive Test History but a Low CD57 NK Count (<60)?

Again, the same procedure was applied but using the LD-Positive and CD57 groups of Table I. Here, two of six pairwise comparisons returned statistically significance between the groups ($p < 0.05$). All three TSD p-values suggested the groups were not different ($p > 0.05$), and the ISREA node set no. 2 TPD pairwise calculation ($p = 0.69$) also suggested the groups were not significantly different. These analyses also suggests that some urine specimens of the CD57 group could have the LD molecular signature. It is noted that several specimens are contained in both the Neg-Test and CD57 groups, so this is logical. Again, the individual specimens were analyzed with the Raman-based screen and chemometric analysis, and results are given later.

Building a Raman-Based Urine Screen for Lyme Disease

Question 5: How Would a Rametrix-Based Urine Screen Perform When Constructed With Urine

Spectra From Lyme Disease-Positive Patients and Healthy Volunteers?

First, the differences between the urine spectra of the LD-Positive group were compared further against those of the Healthy group. This was done with PCA and DAPC using both Goldindec and ISREA baselining (Figure 2). For reference, data point clustering in PCA and DAPC plots indicate spectral (and molecular) similarities. Distance between clusters arises from dissimilarities among groups (defined in Table I) of spectra (e.g., LD-Positive vs Healthy). In addition, PCA is an unsupervised model, meaning only processed Raman spectral data were used as inputs. No classification data (e.g., LD-Positive or Healthy) were considered in PCA. DAPC, however, generates a supervised model, where principal components (PCs) from PCA and classification data were used in model construction. DAPC models must be validated with samples not used in model construction. Here, we used leave-one-out analysis.

The PCA results for Goldindec (Figure 2a) showed some concentration of LD-Positive and Healthy group spectra, but complete separation between clusters was not observed. For a DAPC model built with 29 PCs (Figure 2b) 99.95% of the dataset variance was represented. This led to separation of the LD-Positive urine spectra from those of the Healthy group along the first two canonical axes. By contrast, the unsupervised PCA model built with ISREA node set no. 2 baselined spectra (Figure 2c) led to improved separation of the LD-Positive spectra from those of Healthy. DAPC results with five PCs (Figure 2d) showed slightly worse separation of clusters compared to the DAPC model with Goldindec (Figure 2b). Importantly, this analysis, alone, shows that spectral differences can be found between these two groups of urine spectra and that a unique LD molecular signature may exist. How well these models perform in assigning a group (i.e., LD-Positive or Healthy) to an "unknown" urine specimen is addressed in the following sections. At this point, it is also unclear, but of interest, whether those spectra that separate further from the Healthy cluster represent more "severe" LD-positive cases. PCA and DAPC results given ISREA node set no. 1 are given as Figures S2 and S3 (Supplemental Material) In addition, the PCA data (coefficients, sores, PC loadings) given the three baselining procedures are also available in the Supplemental Material.

Rametrix Pro was applied for leave-one-out analysis of DAPC models. This was done to assess how well the Raman-based analysis would serve as a urine screen to detect a unique spectral signature associated with LD. The details of Rametrix Pro have been published[47] and it has also been used to develop a urine screen for ESKD[44] and BCA.[45] In the leave-one-out analysis, the urine spectrum "left-out" of the model building process was treated as the "unknown" and then assigned to a group (i.e., LD-Positive or Healthy) using the model. The prediction was then compared to its real grouping. This procedure was repeated for all spectra in the dataset. From this, overall model accuracy, sensitivity, PPV, and NPV were calculated.

Several DAPC models were constructed with Goldindec and ISREA baselining of spectra. Leave-one-out analysis was performed for each one with Rametrix Pro, and performance metrics are given in Table III. For Goldindec, the top

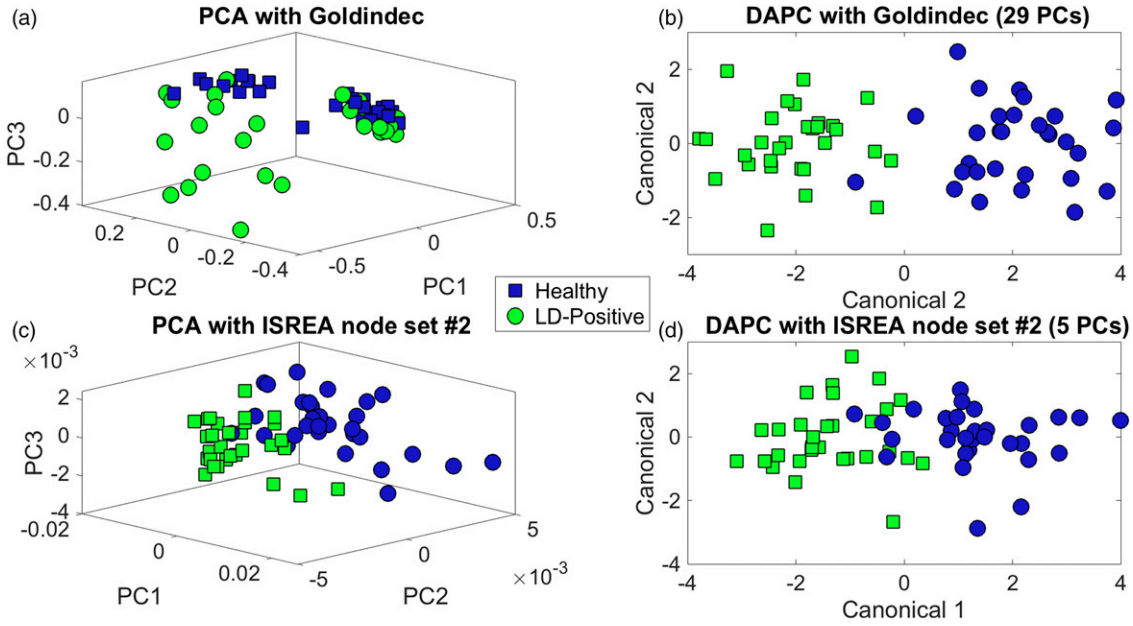

Figure 2. Distinguishing between LD-positive patients and healthy volunteers. (a) PCA results for Goldindec baselining, (b) DAPC using 29 PCs with Goldindec baselining, (c) PCA results for ISREA node set no. 2 baselining, and (d) DAPC using 5 PCs with ISREA baselining with node set no. 2.

Table III. Rametrix PRO results for LD-positive patients and heathy human volunteers using Goldindec and ISREA baselining.

PCs	Dataset variance explained by PCs, %	Accuracy, %	Sensitivity, %	Specificity, %	PPV, %	NPV, %
Golindec baselining						
5	97.9	73.3	63.3	83.3	79.2	69.4
10	99.4	63.3	63.3	63.3	63.3	63.3
20	99.9	51.7	63.3	40.0	51.4	52.2
29	99.95	88.3	83.3	93.3	92.6	84.8
30	99.95	83.3	83.3	83.3	83.3	83.3
40	99.98	53.3	26.7	80.0	57.1	52.2
ISREA baselining (node set no. 1)						
5	97.7	71.7	60.0	83.3	78.3	67.6
10	99.1	71.7	66.7	76.7	74.1	69.7
20	99.7	63.3	63.3	63.3	63.3	63.3
ISREA baselining (node set no. 2)						
5	98.8	86.7	86.7	86.7	86.7	86.7
10	99.6	85.0	76.7	93.3	92.0	80.0
20	99.9	80.0	70.0	90.0	87.5	75.0

performer (over 88% accuracy) was built with 29 PCs, which required 99.95% of the dataset variance. A model built using five PCs (97.9% of the dataset variance) achieved over 73% accuracy. Likewise, a model built with ISREA node set no. 1 and five PCs (97.7% of dataset variance) achieved almost 72% accuracy. However, the ISREA node set no. 2 model with five PCs (98.8% of dataset variance) was able to achieve almost 87% overall accuracy. An assessment of why the ISREA node set no. 2 performed better than node set no. 1 is left for the Discussion section.

The following conditions were used in choosing model(s) to consider in a urine screen for LD. First, all metrics (i.e., accuracy, sensitivity, specificity, PPV, and NPV) had to exceed 50%, with preference given to better performers. Second, the model must be simple (built with few PCs). Models built with more PCs have the potential for over-fitting the dataset, which can lead to poorer performances as more unknown samples are screened. Finally, models that maximized NPV were favored. This minimizes in the incidents of false-positives, which can lead to unnecessary invasive or expensive diagnostic tests and/or treatments.

Elucidating the Molecular Signature of Lyme Disease in Raman Spectra of Urine Specimens

Question 6: What Molecules (i.e., Molecular Signature) Distinguish Lyme Disease Patient Urine From That of Healthy Volunteers?

The identification of spectral contributions leading to separations of clusters in PCA and DAPC can traced to molecular differences between samples. Here, we determined what Raman shift intensities were significantly different among the LD-Positive and Healthy groups of spectra. These differences that are unique to LD comprise its molecular signature in urine. The contribution of each Raman shift to the separations between LD-Positive and Healthy (Figure 2) are given in the Supplemental Material (PC loadings and Figures S4–S9) for both Goldindec and ISREA baselined models. The biological molecules associated with these Raman shifts were identified in a published database.[51,52] The full set of results is given in Supplemental Table S2 in the Supplemental Material, and the most prominent contributions are shown in Table IV. Results include contributions from both PCA and DAPC models and a Significance Score. The Significance Score has a range of 0–6 and is the total number of times a Raman shift was deemed significant in the models analyzed (PCA and DAPC for the Goldindec and two ISREA baselined models). Given our spectral resolution, the average difference between our observed Raman shift and the published values[51,52] was about 0.74 cm^{-1}. Both the observed and the published Raman shifts are given in Table IV and Supplemental Table S2.

A recent metabolomic analysis of urine, using LC-MS for the detection of LD, highlighted the presence of tryptophan and tryptophan metabolites, among others, in the urine of LD-positive patients.[39] Tryptophan was also present as a prominent contributor in our analysis in Table IV. It was found with a Significance Score of four or greater at the following Raman shifts: 622 and 623 cm^{-1} (aromatics more broadly) (score = 5), 873 cm^{-1} (score = 5), 877–880 cm^{-1} (score = 5), and 1622–1624 (score = 5). Tryptophan was also represented in seven more Raman shifts in Supplemental Table S2. Other contributors with a significance score of three or greater included nucleic acids and DNA/RNA (669, 677–680, 618, 628, 804, 1078, 1262, and 1228–1229 cm^{-1}); lipids and triglycerides (1072–1074, 1078, 1262, and 1328–1329 cm^{-1}); sugars (845, 846–847, 993–994, and 1025 cm^{-1}); collagen (669, 1328–1329, and 1635 cm^{-1}); other proteins/peptides (890–892, 979–982, 1243, 1262, 1629, 1633, 1642–1643, 1647–1649, and

Table IV. Prominent Raman shifts[a] leading to differentiation between LD-positive patients and healthy volunteers with a significance score of three or higher.

Observed Raman shift[b] (cm^{-1})	Raman shift (cm^{-1}) in the literature[c]	Assignment(s) and reference(s)[c]	Goldindec (29 PCs)	ISREA node set no. 1 (five PCs)	ISREA node set no. 2 (five PCs)	Significance score[d] (0–6)
			Present in PCA, DAPC, both?			
622, 623	620, 621	Related to aromatics[53–55]	Both	Both	—	4
669	667–669	Collagen type I, DNA/RNA[55–57]	PCA	Both	—	3
677–681	678	DNA[58]	Both	Both	—	4
683–685	—	—	PCA	Both	—	3
804	802	Uracil[59]	PCA	—	Both	3
810–812	812	Phosophodiester[60]	DAPC	—	Both	3
828	828	DNA/RNA[57]	DAPC	—	Both	3
832, 833	831	Tyrosine[58]	DAPC	—	Both	3
845–847	847	Mono- and disaccharides[61]	DAPC	—	PCA	3
873	873	Hydroxyproline, tryptophan[56]	DAPC	Both	Both	5
877–880	880	Tryptophan[61]	DAPC	Both	Both	5
883	883	Protein[62]	—	Both	Both	4
890–892	890	Structural protein modes of tumors[63]	DAPC	—	Both	3
906, 907	906	Tyrosine[64]	DAPC	—	Both	3
979–982	980	β-sheet protein	Both	Both	PCA	5
993, 994	996	Ribose[65]	Both	PCA	Both	5
1002	1002 (experimental Standard)	Urea (dominant in urine)	Both	Both	Both	6
1005	1005	Phenylalanine, protein,[57] carotenoids[66]	—	Both	PCA	3
1025	1025	Carbohydrates,[65] glycogen[67]	DAPC	—	Both	3
1047, 1048	1048	Glycogen[68]	DAPC	Both	Both	5
1072–1074	1073	Triglycerides[69]	DAPC	PCA	Both	4
1078	1078	Phospholipids,[70] nucleic acids[62]	DAPC	Both	Both	5
1262	1263	DNA/RNA, protein, lipids[58,66]	—	PCA	Both	3
1328, 1329	1330	Phospholipids,[63,71] DNA,[63,72] collagen[72]	PCA	Both	—	3
1622–1624	1623	Tryptophan[56]	PCA	Both	Both	5
1629	1628	β-form polypeptides[73]	PCA	Both	Both	5
1633	1634	Amide I[65]	—	Both	Both	4
1635	1635	Collagen[65]	—	Both	Both	4
1642, 1643	1645	Amide I[55]	PCA	Both	Both	5
1647–1649	1650	Amide I[71]	—	Both	Both	4
1653	1653	Carbonyl, amide I[74,75]	—	Both	Both	4

[a]Prominent is defined as having a peak intensity above the tolerance lines shown in the Supplemental Material (Supplemental Figures S4–S9): 0.4% for Goldindec and 0.2% for ISREA.
[b]The observed Raman shift values sometimes differed from the published value following Raman shift calibration based on urea (1002 cm^{-1}). The average deviation was 0.74 cm^{-1}.
[c]All references and Raman shifts given in this table were first reported by Movasaghi et al.[51].
and Talari et al.[52].
[d]The significance score is defined as the total number of models in which the Raman shift is prominent. The range is from zero (no occurrences) to six (prominent in every model).

1653 cm^{-1}); and urea (1002 cm^{-1}). In addition, of the 112 Raman shifts listed in Supplemental Table S2: 17 (15.2%) were associated with lipids; 28 (25%) were associated with aromatics; 17 (15.2%) were associated with nucleic acids; 16 (14.3%) were associated with carbohydrates; 10 (8.9%) mention collagen specifically; three (2.7%) are related to red blood cells; and three (2.7%) are related to carotenoids. In addition, an observed Raman shift at 683–685 cm^{-1} was found with a significance score of three; however, no molecular association has yet been found. Taken together, the prominent Raman shifts in Table IV comprise the majority of our Raman molecular signature of LD. Other minor contributors (for a total of 112 Raman shifts) are shown in Supplemental Table S2.

Testing the Rametrix-Based Lyme Disease Urine Screen Against Other Patient Groups

Question 7: If a Molecular Signature for Lyme Disease is Found, is it Truly Specific for Lyme Disease?

End-stage kidney disease and BCA are two other disease conditions that significantly impact the molecular composition of urine. We have shown previously these can both be resolved using Raman spectroscopy of urine and similar computational approaches.[44,45] Here, we sought to determine whether urine from LD-positive patients could still be resolved when compared against that of ESKD and BCA patients in addition to healthy volunteers. First, we determined whether statistical significance existed among the groups through ANOVA and pairwise comparison calculations with TSD and TPD values. Results are given in Supplemental Table S3. With Goldindec baselining and TPD values, all groups were statistically different ($p < 0.05$), and eight of 10 comparisons returned $p < 0.001$. For ISREA node set no. 1 baselining, all groups were statistically different ($p < 0.001$) except for the Healthy and Surine groups. It is noted again that Surine is a urinalysis control. Finally, for ISREA node set no. 2 baselining, all groups were found statistically different with $p < 0.001$, except for Healthy and Surine ($p = 0.004$). Thus, the LD molecular signature in Raman spectra of urine is statistically different from those of ESKD and BCA.

Next, PCA and DAPC models were constructed, and the results of four DAPC models are shown in Figures 3 and 4: Goldindec baselining with five PCs, Goldindec with 29 PCs, ISREA node set no. 1 with five PCs, and ISREA node set no. 2 with five PCs. DAPC models revealed significant LD-Positive and LD-Negative regions along the first canonical axis for all four models. A layer of overlap also existed, which was considered "inconclusive" to separate LD-positive and LD-negative urine spectra. While the boundaries of the inconclusive region are debatable, it appeared to be smallest in the DAPC model built with ISREA node set no. 2 baselining and five PCs. The analyses were repeated considering LD-Positive, Healthy, ESKD, and BCA groups independently. The DAPC results are shown in Figure 4 for all four models.

Next, leave-one-out analysis was applied to determine the performance of the DAPC models for identifying the presence of LD in an "unknown" urine spectrum, given the expanded set of LD-negative urine specimens. Results are shown in Table V. Here, the DAPC model constructed with five PCs

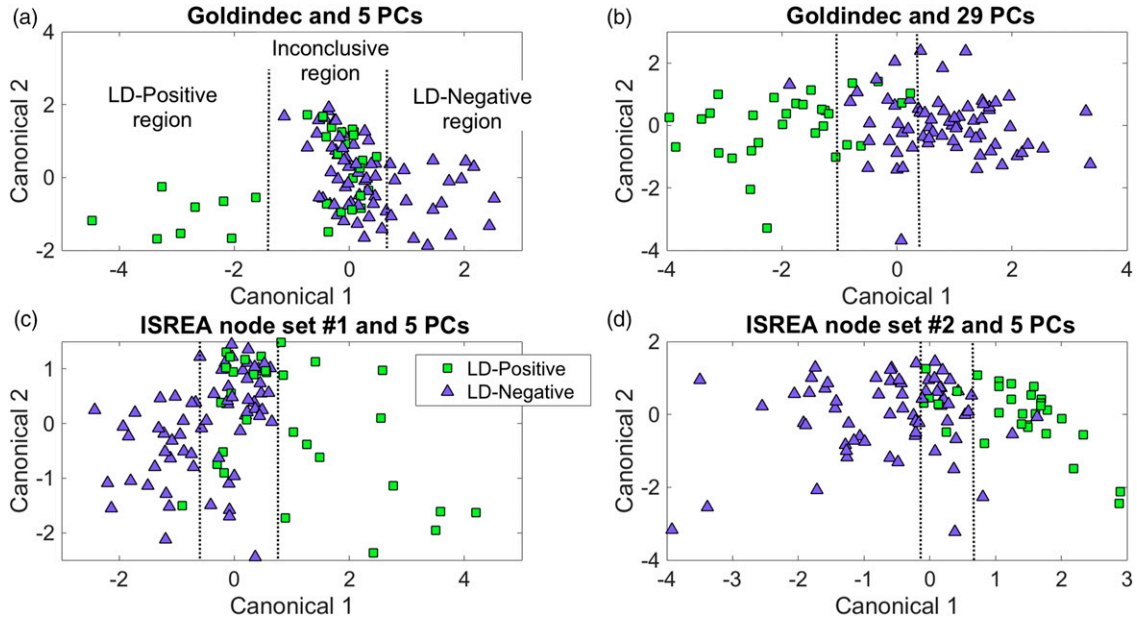

Figure 3. DAPC results for LD-Positive versus LD-Negative (Healthy, ESKD, BCA) for (a) Goldindec baselined data and five PCs to build the DAPC model, (b) Goldindec baselined data and 29 PCs, (c) ISREA node set no. 1 baselined data and five PCs, and (d) ISREA node set no. 2 data and five PCs.

and ISREA node set no. 2 baselining performed best, yielding almost 89% overall accuracy, 80% sensitivity and PPV, and 90% specificity and NPV. The DAPC models built with five PCs and Goldindec or ISREA node set no. 1 baselining performed similarly, with overall accuracies of 70 and 65%, respectively. The DAPC model built with 29 PCs and Goldindec baselining classified few samples as "LD-Positive," leading to a sensitivity of <10%. This showed stark contrast to the results shown in Figures 3b and 4b and suggested this model suffered from overfitting of data. An additional model was constructed with 47 PCs, and this issue appeared rectified, as the overall accuracy approached 80% and sensitivity exceeded 73%. This example demonstrates the potential for model overfitting as the number of PCs used to build DAPC models is increased and the dataset variance explained by PCs nears 100%. Finally, we used the models in attempt to identify if an unknown urine specimen belongs to the Healthy group. Results are given in Table VI and, again, show a superior performance by ISREA node set no. 2 baselining, returning 86.6% overall accuracy.

Question 8: What Percentage of Those Patients With Symptoms Resembling Lyme Disease and Either (i) No Serological Test History or (ii) An Lyme Disease Negative Serological Test Would Screen Positive With the Rametrix-Based Urine Screen?

We applied the Raman-based screens of Table III (LD-Positive vs Healthy groups; called "simple screen") and Table V (LD-Positive versus LD-Negative groups; called "comprehensive screen") to the patients of Table I who had no serological test (No-Test group) and those who had tested negative previously, but still presented with LD-like symptoms (Neg-Test group). For simplicity, we only used ISREA node set no. 2 baselining and DAPC models built with five PCs for these calculations. The percentage of urine specimens that screened positive for LD with each test are given below in Table VII. As shown, the Rametrix-based screens can be used to identify additional patients with a LD molecular signature in urine. The simple screen identified

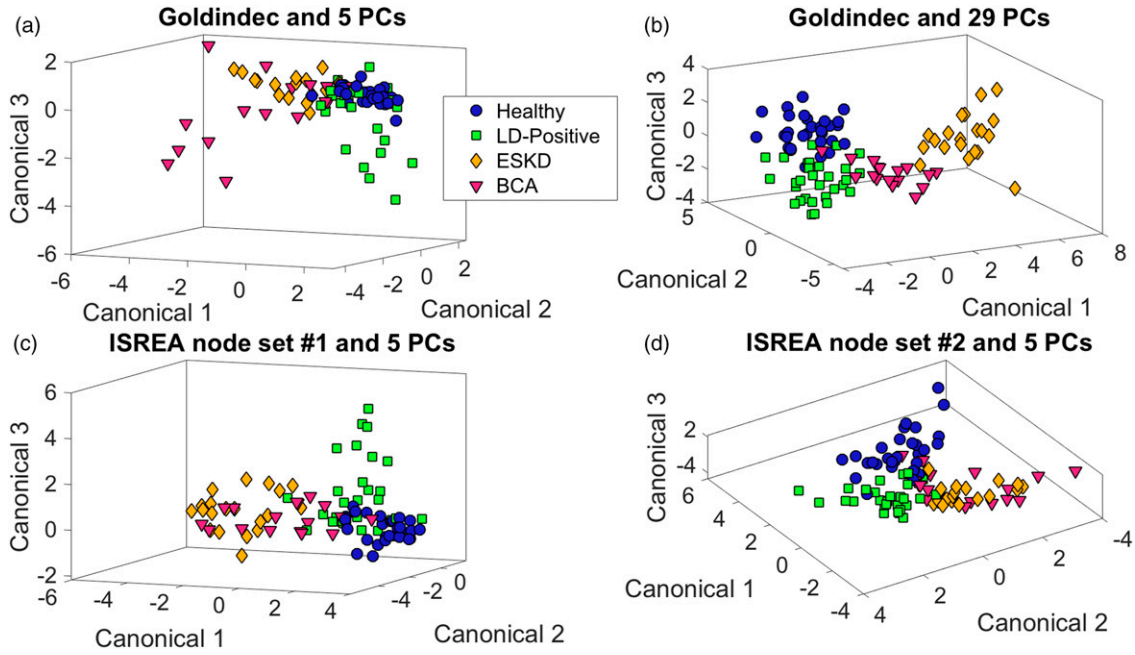

Figure 4. DAPC results for LD-Positive, Healthy, ESKD and BCA datasets, individually, for (a) Goldindec baselined data and five PCs to build the DAPC model, (b) Goldindec baselined data and 29 PCs, (c) ISREA node set no. 1 baselined data and five PCs, and (d) ISREA node set no. 2 data and five PCs.

Table V. Leave-one-out results for identifying LD-positive patients against the LD-Negative group (healthy, ESKD, and BCA).

PCs	Dataset variance explained, %	Accuracy, %	Sensitivity, %	Specificity, %	PPV, %	NPV, %
Goldindec (five PCs)	95.7	70.0	60.0	74.6	51.4	80.7
Goldindec (29 PCs)	99.9	71.1	6.7	100	100	70.5
Goldindec (47 PCs)	99.96	79.4	73.3	82.1	64.7	87.3
ISREA node set no. 1 (five PCs)	96.9	65.0	76.7	59.7	46.0	85.1
ISREA node set no. 2 (five PCs)	98.5	88.7	83.3	91.0	80.7	92.4

Table VI. Leave-one-out results for identifying healthy volunteers against LD-positive, ESKD, and BCA patients.

PCs	Dataset variance explained, %	Accuracy, %	Sensitivity	Specificity, %	PPV	NPV, %
Goldindec (five PCs)	95.7	80.4	86.7%	77.6	63.4%	92.9
Goldindec (29 PCs)	99.9	69.1	N/A	100	N/A	69.1
Goldindec (47 PCs)	99.96	79.4	60.0%	88.1	69.2%	83.1
ISREA node set no. 1 (five PCs)	96.9	82.5	90.0%	79.1	65.9%	94.6
ISREA node set no. 2 (five PCs)	98.5	86.6	86.7%	86.6	74.3%	93.6

Table VII. Percentage of the No-Test and Neg-Test groups screening positive for LD with the simple and comprehensive Rametrix-based urine screens.

	Simple screen[a], %	Comprehensive screen[b], %
No-test group	75.6	65.9
Neg-test group	53.8	30.8

[a]The simple screen is composed of LD-Positive and Healthy groups (Table III).
[b]The comprehensive screen is composed of LD-Positive and LD-Negative groups (Table V).

more of these urine specimens and belonging to the LD-Positive group, suggesting that the comprehensive screen is more selective. With this, over 30% tested positive for LD by the Rametrix-based urine screen who had tested negative by other means previously. In addition, over 65% of patients who did not receive a previous test showed the LD molecular signature in their urine specimen. Graphical views of clustering in DAPC plots in the presence of unknowns are given in Supplemental Figure S10.

Discussion

Major findings from our study are summarized as follows. Patients who were seropositive by the two-tier CDC standard diagnostic test for LD had statistically significant changes in the molecular composition of their urine that differentiated them from normal, healthy individuals, as determined by Raman spectroscopy and Rametrix analyses of urine specimens; the molecular signature of LD in urine is complex, comprising more than 31 Raman shifts with major contributions and several more with minor contributions; urine specimens from patients who were considered to be LD-positive with other laboratory tests (not the two-tier CDC standard diagnostic test) were statistically similar to specimens of urine from patients who tested positive with the CDC standard two-tier test; several patients who were LD-negative (with two-tier or other LD diagnostic tests) had urine spectral changes similar to those who were LD-positive, but it is possible they had been previously infected but were not reactive at the time of assay (i.e., presented for long-term chronic fatigue); the molecular changes seen in the urine of LD-positive patients was not only statistically different from the urine of normal, healthy individuals, but also from the urine of patients with other genitourinary tract pathologies, including ESKD and BCA, suggesting the LD-associated urine molecular signature appears to be unique.

Raman spectral baselining procedures can play a critical role in chemometric analyses. Here, we found the Goldindec algorithm and ISREA could both locate a molecular signature for LD. ISREA was able to return similar or better prediction accuracies in DAPC models with fewer PC inputs.

With ISREA, the location of node placements is critical and can impact chemometric model performance.

As noted in the Introduction to this paper, current serodiagnostic methods for diagnosis of LD fall short of needs (rapid and early detection), may have unsatisfactory sensitivity/specificity/predictive value,[76] can be costly (>$200), and require multiple invasive blood collections over a period of several weeks.

There have been a number of studies, over the past 30 years, which have reported changes in the composition of urine that may have reflected the presence of LD. Early studies[40,41] looked for pathogen-related proteins in urine; these studies were not sufficiently definitive to result in laboratory use, but did encourage continued investigation that could lead (eventually) to clinical application of these methods. Magni et al.[42] showed that a molecular marker, the outer surface protein A C-terminus peptide (OspA), of the pathogen could be detected in the urine of patients with early, active infections with nanotrap technology. Levels of OspA declined with clinical recovery, suggesting that this testing procedure could have value in detection and management of early infections (i.e., use or non-use of antibiotics). This test has been commercialized (Nanotrap, Ceres Nanoscience, USA); the extent of clinical use is difficult to discern from the literature. The recent study by Pegalajar-Jurado et al.[39] showed that LD urine could be differentiated from non-LD urine using advanced metabolomic analysis, using liquid chromatography/mass spectroscopy. In the Pegalaiar-Jurado et al.[39] study, changes in metabolism, related to infection, were shown by alterations in urine metabolites (including alterations in tryptophan metabolism). These findings agreed with our observations, which identified changes tryptophan and other aromatic compounds as part of the LD molecular signature.

Thus, access to a simple, rapid, economical, noninvasive, and accurate test would be a significant and meaningful step in detection and management of LD. We believe the Rametrix-based urine screening procedure, described here, fulfills these needs. Our data show that a molecular signature, associated with serologically confirmed LD, can be detected, and this

molecular signature differentiates LD from urine specimens of healthy individuals and from specimens of patients with genitourinary pathologies, such as ESKD or BCA. Of course, molecular signatures for other diseases (e.g., proteinuria and urinary tract infections, among others) likely exist and could be elucidated in future research. The extent to which these may overlap with the LD molecular signature remains unknown at this point. Broad comprehensive databases of urine Raman spectra representing many pathologies would be useful for this purpose. The research presented here is one of the first proofs of concept of this approach to our knowledge.

Urine specimen collection (free catch) simply requires urinating into a cup. Samples can be stored at room temperature for up to 12 h before analysis. No processing (i.e., addition of chemical preservatives or centrifugation) of the urine specimen is needed and total time required to scan the sample repetitively (10–15 repeat scans/sample) and generate a spectrum for computational analysis is <15 min, including sample handling time (transfer from urine collection cup to 1.5 mL sample vial). A miniscule (<2 mL) volume of urine is required for analysis and scanning is nondestructive. Samples can be stored at low temperatures (<–30 °C for >30 days), thawed and then scanned/re-scanned, as needed.[45] Technical personnel can be trained in a few hours to analyze specimens. The Raman spectrometers used for these analyses are inexpensive (<US$ 20 000) and are commercially available. Clearly, the capital and personnel costs of running Raman-based assays in laboratory settings are modest (approximately US$50/sample), in comparison to urine metabolomic screening (~US$400/sample), and serodiagnostic testing (>US$200/sample).

Our results are based on robust computational/statistical analysis of Raman spectra and capitalize on our ability to compare the characteristics of these spectra (at hundreds of different Raman shifts) with extensive libraries of Raman chemical reference spectra,[77] urine metabolomics,[78] and our own Raman databases (235 normal, that is, healthy adult; 455 ESKD; and 74 BCA urine Raman spectra). We feel that access to this database of specimens was a key to detecting statistically meaningful results that we report here.

We are currently collecting data from more LD-positive and LD-negative patients and conducting studies to further identify major contributors to the LD molecular signature and to enroll more LD-positive and LD-negative patients. We acknowledge the ongoing controversies surrounding the contribution of LD infection to persons experiencing chronic fatigue. We believe the results of the current study are indicative of a currently undefined systemic reaction to LD infection, but we fully expect this systemic reaction could be seen with other pathologies (e.g., myalgic encephalomyelitis/chronic fatigue syndrome, proteinuria, and post-acute COVID-19 long haul syndrome). We hope that our methods may be used to help identify patients who would benefit from various therapies directed at LD management, but also other infectious or environmental diseases (e.g., other tick-borne diseases, mold exposure, COVID-19, etc.). Our ongoing work is also directed at determining if co-morbidities may affect the LD molecular signature and results returned by the Rametrix-based analysis.

Finally, from the point of view of the chemometric analyses performed in this study, we found both Goldindec and ISREA baselining beneficial, and we note that several of our prior studies have made use of the Goldindec algorithm. Minimizing the number of PCs used in building DAPC models has shown, in our studies, to be beneficial to predicting outcomes of unknown urine specimens. The ISREA baselining algorithm was published recently,[48] and much is still being learned about its capabilities and use in chemometric analyses. In this study, it allowed for similar or better predictive capabilities with DAPC models with fewer PC inputs. However, this was dependent on node placement, as evidenced by comparing results from node sets no. 1 and no. 2. How the number of nodes is selected and how they are placed most effectively remains a topic of future research. In the current study, we found that the absence of nodes from ~1400–1800 cm^{-1} in ISREA node set no. 2 enhanced that region of the spectrum, and a higher concentration of nodes from 600–1000 cm^{-1} allowed the elimination of Raman shifts possibly unrelated to LD (Supplemental Figure S1).

Conclusion

Here, we present results of studies conducted to determine if Raman spectroscopy and Rametrix analysis of urine would serve as a suitable screen for LD. Our results indicate there are statistically significant changes in the urine of patients who test positive for LD when their urine molecular composition is compared to that of normal, healthy volunteers or patients with genitourinary tract pathology. We believe our methods could be easily applied as an accurate, rapid, and inexpensive urine screen for LD.

Acknowledgments

We acknowledge contributions of ASI in the revision of this manuscript.

Declaration of Conflicting Interests

The authors declared the following potential conflicts of interest with respect to the research, authorship, and/or publication of this article: RSS and JLR co-founded DialySensors, Inc., to commercialize the detection of Lyme disease in urine and have filed US patent application 17/146301. DialySensors also seeks to trademark Rametrix.

Funding

The authors received no financial support for the research, authorship, and/or publication of this article.

ORCID iD

Ryan Senger https://orcid.org/0000-0002-2450-6693
John Robertson https://orcid.org/0000-0003-4361-999X

Supplemental Material

All supplemental material mentioned in the text is available in the online version of the journal.

References

1. J.L. Benach, E.M. Bosler, J.P. Hanrahan, et al. "Spirochetes Isolated From the Blood of Two Patients With Lyme Disease". N. Engl. J. Med. 1983. 308(13): 740–742. doi: 10.1056/NEJM198303313081302.
2. A.C. Steere, S.E. Malawista, NH. Bartenhagen, et al. "The Clinical Spectrum and Treatment of Lyme Disease". Yale J. Biol. Med. 1984. 57(4): 453–461.
3. A.C. Steere, R.L. Grodzicki, J.E. Craft, et al. "Recovery of Lyme Disease Spirochetes From Patients". Yale J. Biol. Med. 1984. 57(4): 557–560.
4. W. Burgdorfer. "Discovery of the Lyme Disease Spirochete and Its Relation to Tick Vectors". Yale J. Biol. Med. 1984. 57(4): 515–520.
5. L.A. Waddell, J. Greig, M. Mascarenhas, et al. "The Accuracy of Diagnostic Tests for Lyme Disease in Humans, A Systematic Review and Meta-Analysis of North American Research". PLoS One. 2016. 11(12): e0168613). doi: 10.1371/journal.pone.0168613.
6. A.M. Kilpatrick, A.D.M. Dobson, T. Levi, et al. "Lyme Disease Ecology in a Changing World: Consensus, Uncertainty and Critical Gaps for Improving Control". Philos. Trans. R. Soc. Lond. 2017. 372(1722): 20160117. doi: 10.1098/rstb.2016.0117.
7. Centers for Disease Control and Prevention. "Lyme Disease Data Tables: Most Recent Year. Lyme Disease. CDC". 2019. https://www.cdc.gov/lyme/datasurveillance/tables-recent.html [accessed Feb 19 2021].
8. R.D. Evans, E.M. Bosler, F. Orthel, et al. "Canine Lyme Borreliosis: I Gross Clinical Observations of Laboratory Beagles Following Exposure to Ticks Infected with *Borrelia burgdorferi*". J. Spirochetal Tick-Borne Dis. 1995. 2(2): 28–32.
9. R.D. Evans, J.L. Robertson, M.D. Graham, et al. "Canine Lyme Borreliosis II: Minimal Lesions in Tissues of Laboratory Beagles Following Infection by Exposure to Ixodid Ticks Infected with *Borrelia burgdorferi*". J. Spirochetal Tick-Borne Dis. 1995. 2(2): 33–36.
10. T.J. Divers, R.B. Gardner, J.E. Madigan, et al. "*Borrelia burgdorferi* Infection and Lyme Disease in North American Horses: A Consensus Statement". J. Vet. Intern. Med. 2018. 32(2): 617–632. doi: 10.1111/jvim.15042.
11. M.P. Littman, R.E. Goldstein, M.A. Labato, et al. "ACVIM Small Animal Consensus Statement on Lyme Disease in Dogs: Diagnosis, Treatment, and Prevention". J. Vet. Intern. Med. 2006. 20(2): 422–434. doi: 10.1892/0891-6640(2006)20[422:asacso]2.0.Co;2.
12. A.C. Steere, S.E. Malawista, D.R. Snydman, et al. "Lyme Arthritis: An Epidemic of Oligoarticular Arthritis in Children and Adults in Three Connecticut Communities". Arthritis Rheum. 1977. 20(1): 7–17. doi: 10.1002/art.1780200102.
13. G. Stanek, G.P. Wormser, J. Gray, et al. "Lyme Borreliosis". Lancet. 2012. 379(9814): 461–473. doi: 10.1016/S0140-6736(11)60103-7.
14. A.C. Steere, F. Strle, G.P. Wormser, et al. "Lyme Borreliosis". Nat. Rev. Dis. Primer. 2016. 2: 16090. doi: 10.1038/nrdp.2016.90.
15. E.R. Adrion, J. Aucott, K.W. Lemke, et al. "Health Care Costs, Utilization and Patterns of Care Following Lyme Disease". PLoS One. 2015. 10(2): e0116767. doi: 10.1371/journal.pone.0116767.
16. P.M. Lantos, L.E. Nigrovic, P.G. Auwaerter, et al. "Geographic Expansion of Lyme Disease in the Southeastern United States, 2000–2014". Open Forum Infect. Dis. 2015. 2(4): ofv143. doi: 10.1093/ofid/ofv143.
17. B.L. Stone, Y. Tourand, C.A. Brissette. "Brave New Worlds: The Expanding Universe of Lyme Disease". Vector Borne Zoonotic Dis. 2017. 17(9): 619–629. doi: 10.1089/vbz.2017.2127.
18. M. Davidsson. "The Financial Implications of a Well-Hidden and Ignored Chronic Lyme Disease Pandemic". Healthcare. 2018. 6(1): 16. doi: 10.3390/healthcare6010016.
19. V.K. Lloyd, R.G. Hawkins. "Under-Detection of Lyme Disease in Canada". Healthcare. 2018. 6(4): 125. doi: 10.3390/healthcare6040125.
20. A. DeLong, M. Hsu, H. Kotsoris. "Estimation of Cumulative Number of Post-Treatment Lyme Disease Cases in the US, 2016 and 2020". BMC Public Health. 2019. 19(1): 352. doi: 10.1186/s12889-019-6681-9.
21. A.F. Hinckley, N.P. Connally, J.I. Meek, et al. "Lyme Disease Testing by Large Commercial Laboratories in the United States". Clin. Infect. Dis. Off. Publ. Infect. Dis. Soc. Am. 2014. 59(5): 676–681. doi: 10.1093/cid/ciu397.
22. Centers for Disease Control and Prevention (CDC). "Signs and Symptoms of Untreated Lyme Disease". 2019. https://www.cdc.gov/lyme/signs_symptoms/ [accessed Nov 5 2021].
23. L.E. Nigrovic, J.E. Bennett, F. Balamuth, et al. "Accuracy of Clinician Suspicion of Lyme Disease in the Emergency Department". Pediatrics. 2017. 140(6): e20171975. doi: 10.1542/peds.2017-1975.
24. P.M. Lantos, J.A. Branda, J.C. Boggan, et al. "Poor Positive Predictive Value of Lyme Disease Serologic Testing in an Area of Low Disease Incidence". Clin. Infect. Dis. Off. Publ. Infect. Dis. Soc. Am. 2015. 61(9): 1374–1380. doi: 10.1093/cid/civ584.
25. P.M. Lantos. "Chronic Lyme Disease". Infect. Dis. Clin. North Am. 2015. 29(2): 325–340. doi: 10.1016/j.idc.2015.02.006.
26. T. Kobayashi, Y. Higgins, R. Samuels, et al. "Misdiagnosis of Lyme Disease With Unnecessary Antimicrobial Treatment Characterizes Patients Referred to an Academic Infectious Diseases Clinic". Open Forum Infect. Dis. 2019. 6(7): ofz299. doi: 10.1093/ofid/ofz299.
27. L. Johnson, M. Shapiro, R.B. Stricker, et al. "Antibiotic Treatment Response in Chronic Lyme Disease: Why Do Some Patients Improve While Others Do Not?" Healthcare. 2020. 8(4): 383. doi: 10.3390/healthcare8040383.
28. LymeDisease.org "MyLymeData101". LymeDisease.Org, 2021. https://www.lymedisease.org/mylymedata-101-lyme-disease-research/ [accessed Feb 19 2021].
29. Centers for Disease Control and Prevention (CDC). Signs and Symptoms of Lyme Disease CDC". Centers for Disease Control and Prevention, 2021. https://www.cdc.gov/lyme/signs_symptoms/index.html [accessed Feb 19 2021].

30. M.E. Aguero-Rosenfeld, G.P. Wormser. "Lyme Disease: Diagnostic Issues and Controversies". Expert Rev. Mol. Diagn. 2015. 15(1): 1–4. doi: 10.1586/14737159.2015.989837.
31. R.B. Stricker, E.E. Winger. "Decreased CD57 Lymphocyte Subset in Patients with Chronic Lyme Disease". Immunol Lett. 2001. 76(1): 43–48. doi: 10.1016/s0165-2478(00)00316-3.
32. R.B. Stricker, J. Burrascano, E. Winger. "Longterm Decrease in the CD57 Lymphocyte Subset in a Patient With Chronic Lyme Disease". Ann. Agric. Environ. Med. 2002. 9(1): 111–113.
33. A. Marques, M.R. Brown, T.A. Fleisher. "Natural Killer Cell Counts Are Not Different Between Patients with Post-Lyme Disease Syndrome and Controls". Clin. Vaccin. Immunol. 2009. 16(8): 1249–1250. doi: 10.1128/CVI.00167-09.
34. J.A. Branda, B.A. Body, J. Boyle, et al. "Advances in Serodiagnostic Testing for Lyme Disease Are at Hand". Clin. Infect. Dis. 2018. 66(7): 1133–1139. doi: 10.1093/cid/cix943.
35. A.R. Marques. "Revisiting the Lyme Disease Serodiagnostic Algorithm: The Momentum Gathers". J. Clin. Microbiol. 2018. 56(8): e00749. doi: 10.1128/JCM.00749-18.
36. M.J. Soloski, L.A. Crowder, L.J. Lahey, et al. "Serum Inflammatory Mediators as Markers of Human Lyme Disease Activity". PLoS One. 2014. 9(4): e93243. doi: 10.1371/journal.pone.0093243.
37. A. Moore, C. Nelson, C. Molins, et al. "Current Guidelines, Common Clinical Pitfalls, and Future Directions for Laboratory Diagnosis of Lyme Disease, United States" Emerg. Infect. Dis. 2016. 22(7). doi: 10.3201/eid2207.151694.
38. S.E. Schutzer, B.A. Body, J. Boyle, et al. "Direct Diagnostic Tests for Lyme Disease". Clin. Infect. Dis. 2019. 68(6): 1052–1057. doi: 10.1093/cid/ciy614.
39. A. Pegalajar-Jurado, B.L. Fitzgerald, M.N. Islam, et al. "Identification of Urine Metabolites as Biomarkers of Early Lyme Disease". Sci. Rep. 2018. 8(1): 12204. doi: 10.1038/s41598-018-29713-y.
40. F.W. Hyde, R.C. Johnson, T.J. White, et al. "Detection of Antigens in Urine of Mice and Humans Infected With *Borrelia burgdorferi*, Etiologic Agent of Lyme Disease". J. Clin. Microbiol. 1989. 27(1): 58–61.
41. C. Rauter, M. Mueller, I. Diterich, et al. "Critical Evaluation of Urine-Based PCR Assay for Diagnosis of Lyme Borreliosis". Clin. Diagn. Lab. Immunol. 2005. 12(8): 910–917. doi: 10.1128/CDLI.12.8.910-917.2005.
42. R. Magni, B.H. Espina, K. Shah, et al. "Application of Nanotrap Technology for High Sensitivity Measurement of Urinary Outer Surface Protein A Carboxyl-Terminus Domain in Early Stage Lyme Borreliosis". J. Transl. Med. 2015. 13: 346. doi: 10.1186/s12967-015-0701-z.
43. R.S. Senger, V. Kavuru, M. Sullivan, et al. "Spectral Characteristics of Urine Specimens from Healthy Human Volunteers Analyzed Using Raman Chemometric Urinalysis (Rametrix)". PLoS One. 2019. 14(9): e0222115. doi: 10.1371/journal.pone.0222115.
44. R.S. Senger, M. Sullivan, A. Gouldin, et al. "Spectral Characteristics of Urine From Patients With End-Stage Kidney Disease Analyzed Using Raman Chemometric Urinalysis (Rametrix)". PLoS One. 2020. 15(1): e0227281. doi: 10.1371/journal.pone.0227281.
45. H.M. Huttanus, T. Vu, G. Guruli, et al. "Raman Chemometric Urinalysis (Rametrix) as a Screen for Bladder Cancer". PLoS One. 2020. 15(8): e0237070. doi: 10.1371/journal.pone.0237070.
46. A.K. Fisher, W.F. Carswell, A.I.M. Athamneh, et al. "The Rametrix Lite Toolbox v1.0 for Matlab". J. Raman Spectrosc. 2018. 49(5): 885–896. doi: 10.1002/jrs.5348.
47. R.S. Senger, J.L. Robertson. "The Rametrix PRO Toolbox v1.0 for MATLAB". PeerJ. 2020. 8, e8179. doi: 10.7717/peerj.8179.
48. Y. Xu, P. Du, R. Senger, et al. "An Efficient Peak-Preserving Baseline Correction Algorithm for Raman Spectra". Appl. Spectrosc. 2021. 75(1): 34–45. doi: 10.1177/0003702820955245.
49. J. Liu, J. Sun, X. Huang, et al. "Goldindec: A Novel Algorithm for Raman Spectrum Baseline Correction". Appl. Spectrosc. 2015. 69(7): 834–842. doi: 10.1366/14-07798.
50. R. Trevethan. "Sensitivity, Specificity, and Predictive Values: Foundations, Pliabilities, and Pitfalls in Research and Practice". Front. Pub. Health. 2017. 5: 307. doi: 10.3389/fpubh.2017.00307.
51. Z. Movasaghi, S. Rehman, I. U. Rehman. "Raman Spectroscopy of Biological Tissues". Appl. Spectrosc. Rev. 2007. 42(5): 493–541. doi: 10.1080/05704920701551530.
52. A.C.S. Talari, Z. Movasaghi, S. Rehman, et al. "Raman Spectroscopy of Biological Tissues". Appl. Spectrosc. Rev. 2015. 50(1): 46–111. doi: 10.1080/05704928.2014.923902.
53. E.Ó. Faoláin, M.B. Hunter, J.M. Byrne, et al. "A Study Examining the Effects of Tissue Processing on Human Tissue Sections Using Vibrational Spectroscopy". Vib. Spectrosc. 2005. 38(1): 121–127. doi: 10.1016/j.vibspec.2005.02.013.
54. N. Stone, C. Kendall, N. Shepherd, et al. "Near-Infrared Raman Spectroscopy for the Classification of Epithelial Pre-Cancers and Cancers". J. Raman Spectrosc. 2002. 33(7): 564–573. doi: 10.1002/jrs.882.
55. N. Stone, C. Kendall, J. Smith, et al. "Raman Spectroscopy for Identification of Epithelial Cancers". Faraday Discuss. 2004. 126: 141–157. doi: 10.1039/b304992b.
56. W.-T. Cheng, M.-T. Liu, H.-N. Liu, et al. "Micro-Raman Spectroscopy Used to Identify and Grade Human Skin Pilomatrixoma". Microsc. Res. Tech. 2005. 68(2): 75–79. doi: 10.1002/jemt.20229.
57. Z. Liu, C. Davis, W. Cai, et al. "Circulation and Long-Term Fate of Functionalized, Biocompatible Single-Walled Carbon Nanotubes in Mice Probed by Raman Spectroscopy". Proc. Natl. Acad. Sci. USA. 2008. 105(5): 1410–1415. doi: 10.1073/pnas.0707654105.
58. J.W. Chan, D.S. Taylor, T. Zwerdling, et al. "Micro-Raman Spectroscopy Detects Individual Neoplastic and Normal Hematopoietic Cells". Biophys. J. 2006. 90(2): 648–656. doi: 10.1529/biophysj.105.066761.
59. C. Kendall, J. Day, J. Hutchings, et al. "Evaluation of Raman Probe for Oesophageal Cancer Diagnostics". Analyst. 2010. 135(12): 3038–3041. doi: 10.1039/c0an00536c.
60. A.J. Ruiz-Chica, M.A. Medina, F. Sánchez-Jiménez, et al. "Characterization by Raman Spectroscopy of Conformational Changes on Guanine-Cytosine and Adenine-Thymine Oligonucleotides Induced by Aminooxy Analogues of Spermidine". J. Raman Spectrosc. 2004. 35(2): 93–100. doi: 10.1002/jrs.1107.

61. G. Shetty, C. Kendall, N. Shepherd, et al. "Raman Spectroscopy: Elucidation of Biochemical Changes in Carcinogenesis of Oesophagus". Br. J. Cancer. 2006. 94(10): 1460–1464. doi: 10.1038/sj.bjc.6603102.
62. T. Bhattacharjee, P. Kumar, G. Maru, et al. "Swiss Bare Mice: A Suitable Model for Transcutaneous *In Vivo* Raman Spectroscopic Studies of Breast Cancer". Lasers Med. Sci. 2014. 29(1): 325–333. doi: 10.1007/s10103-013-1347-9.
63. U. Utzinger, D.L. Heintzelman, A. Mahadevan-Jansen, et al. "Near-Infrared Raman Spectroscopy for In Vivo Detection of Cervical Precancers". Appl. Spectrosc. 2001. 55(8): 955–959.
64. X. Li, T. Yang, S. Li, et al. "Surface-Enhanced Raman Spectroscopy Differences of Saliva Between Lung Cancer Patients and Normal People". In: Proceedings of SPIE-OSA Biomedical Optics (Optical Society of America, 2011), Munich, Germany, 22–26 May 2011, 2011. Paper no. 808722.
65. R.K. Dukor. "Vibrational Spectroscopy in the Detection of Cancer". In: J.M. Chalmers, P.R. Griffiths, editors. Handbook of Vibrational Spectroscopy. Chichester, UK: Wiley, 2006. doi: 10.1002/0470027320.s8107.
66. S.M. Ronen, A. Stier, H. Degani. "NMR Studies of the Lipid Metabolism of T47D Human Breast Cancer Spheroids". FEBS Lett. 1990. 266(1–2): 147–149. doi: 10.1016/0014-5793(90)81526-t.
67. R. Mehrotra, D.K. Jangir, S. Agarwal, et al. "Interaction Studies of Anticancer Drug Lomustine With Calf Thymus DNA Using Surface Enhanced Raman Spectroscopy". MAPAN. 2013. 28(4): 273–277. doi: 10.1007/s12647-013-0086-5.
68. J. Binoy, J.P. Abraham, I.H. Joe, et al. "NIR-FT Raman and FT-IR Spectral Studies andab Initio Calculations of the Anti-Cancer Drug Combretastatin-A4". J. Raman Spectrosc. 2004. 35(11): 939–946. doi: 10.1002/jrs.1236.
69. L. Silveira, S. Sathaiah, R.A. Zângaro, et al. "Correlation Between Near-Infrared Raman Spectroscopy and the Histopathological Analysis of Atherosclerosis in Human Coronary Arteries. Lasers Surg. Med. 2002. 30(4): 290–297. doi: 10.1002/lsm.10053.
70. Z. Huang, A. McWilliams, H. Lui, et al. "Near-Infrared Raman Spectroscopy for Optical Diagnosis of Lung Cancer". Int. J. Cancer. 2003. 107(6): 1047–1052. doi: 10.1002/ijc.11500.
71. R. Malini, K. Venkatakrishna, J. Kurien, et al. "Discrimination of Normal, Inflammatory, Premalignant, and Malignant Oral Tissue: A Raman Spectroscopy Study". Biopolymers. 2006. 81(3): 179–193. doi: 10.1002/bip.20398.
72. H. Schulz, M. Baranska. "Identification and Quantification of Valuable Plant Substances by IR and Raman Spectroscopy". Vib. Spectrosc. 2007. 43(1): 13–25. doi: 10.1016/j.vibspec.2006.06.001.
73. R.A. Shaw, H.H. Mantsch. "Vibrational Biospectroscopy: From Plants to Animals to Humans. A Historical Perspective". J. Mol. Struct. 1999. 480: 1–13. doi: 10.1016/S0022-2860(98)00648-6.
74. N. Huang, M. Short, J. Zhao, et al. "Full Range Characterization of the Raman Spectra of Organs in a Murine Model". Opt. Express. 2011. 19(23): 22892–22909. doi: 10.1364/OE.19.022892.
75. S. Farquharson, C. Shende, F.E. Inscore, et al. "Analysis of 5-Fluorouracil in Saliva Using Surface-Enhanced Raman Spectroscopy". J. Raman Spectrosc. 2005. 36(3): 208–212. doi: 10.1002/jrs.1277.
76. G.P. Wormser, A. Levin, S. Soman, et al. "Comparative Cost-Effectiveness of Two-Tiered Testing Strategies for Serodiagnosis of Lyme Disease With Noncutaneous Manifestations". J. Clin. Microbiol. 2013. 51(12): 4045–4049. doi: 10.1128/JCM.01853-13.
77. Y. El Mendili, A. Vaitkus, A. Merkys, et al. "Raman Open Database: First Interconnected Raman-X-Ray Diffraction Open-Access Resource for Material Identification". J. Appl. Crystallogr. 2019. 52(3): 618–625. doi: 10.1107/S1600576719004229.
78. S. Bouatra, F. Aziat, R. Mandal, et al. "The Human Urine Metabolome". PLoS One. 2013. 8(9): e73076. doi: 10.1371/journal.pone.0073076.